http://journal.uir.ac.id/index.php/JGEET

E-ISSN : 2541-5794
P-ISSN : 2503-216X

Journal of Geoscience,
Engineering, Environment, and Technology
Vol 08 No 02 2023

RESEARCH ARTICLE

Hydrocarbon Spectra Slope (HYSS): A Spectra Index for Quantifying and Characterizing Hydrocarbon oil on Different Substrates Using Spectra Data

Kamorudeen Tunde Olagunju [1,*], Callen Scott Allen[2], Samuel Bamidele Olobaniyi[1] , Kayode Festus Oyedele[1]

[1] *Department of Geosciences, University of Lagos, Lagos, Nigeria*

[2] *Department of Geography, University of Mary Washington, Fredericksburg, VA, USA*.

* Corresponding author : kolagunju@unilag.edu.ng.
Tel.:+234-803-716-8057
Received: June 17, 2022; Accepted: June 25, 2023
DOI: 10.25299/jgeet.2023.8.2.9741

Abstract

Many sensors in Optical domain allow for detection of hydrocarbons in oil spills study. However, high resolution laboratory and airborne imaging spectrometers have shown potential for quantification and characterization of hydrocarbon. Available methods in literature for quantifying and characterizing hydrocarbons on these data relies mainly on shapes and positions of hydrocarbon key absorption features, mainly at 1.73 µm and 2.30 µm. Shapes formed by these absorption features are often influenced by spectral features of background substrates, thereby limiting the quality of results. Furthermore, multispectral sensors cannot resolve the shapes of key absorption features, a strong limitation for methods used in previous works. In this study, we present Hydrocarbon Spectra Slope (HYSS), a new spectra index that offers predictive quantification and characterization of common hydrocarbon oils. Slope values for the studied hydrocarbon oils enable clear discrimination for relative quantitative analysis of oil abundance classes and qualitative discrimination for common hydrocarbons on common background substrates. Data from ground-based spectrometers and Airborne Visible/Infrared Imaging Spectrometer (AVIRIS) are resampled to AVIRIS, Advanced Space-borne Thermal Emission and Reflection Radiometer (ASTER) and LANDSAT 7 Enhanced Thematic Mapper's (ETM+) Full Width at Half Maximum (FWHM), in order to compute spectra slope values for hydrocarbon abundance /hydrocarbon-substrate characterization. Despite limitations of nonconformity of central wavelengths and/or band widths of multispectral sensors to key hydrocarbon band, statistical significance for both quantitative and qualitative analysis at 95% confidence level (P-value <0.01) suggests strong potential of the use of HYSS, multispectral and hyperspectral sensors as emergency response tools for hydrocarbon mapping.

Keywords: Hydrocarbon, Oil spill, Hyperspectral, Multispectral

1. Introduction

Hyperspectral sensors for airborne survey and laboratory experiments possess high to very high spectral and spatial resolution. With these sensors, recent studies have revealed the potential of optical remote sensing for oil spill monitoring programs (Fingas and Brown 2017, Holmes, Graettinger, and MacDonald 2017). Hydrocarbons exhibit unique spectral signatures particularly in the Short Wave Infrared Region (SWIR); at 1.73 µm and 2.30 µm wavelength position (Clark et al. 2010, Kühn, Oppermann, and Hörig 2004a). These absorption features correspond to overtones and combination bands common in hydrocarbon compounds. Absorption features at these wavelength positions and in the visible Near Infrared Region (VNIR) at 1.20 µm, are useful for detecting and characterizing hydrocarbon oil (Wettle et al. 2009, Liu et al. 2016, Lu et al. 2013, Andreou and Karathanassi 2011, Kühn, Oppermann, and Hörig 2004b, Reséndez-Hernández, Prudencio-Csapek, and Lozano-García 2018, Asadzadeh and de Souza Filho 2016, Lammoglia and Souza Filho 2012b). However, absorption features in the SWIR provide distinct potential for quantification and characterization of hydrocarbon oil against different background materials (Lammoglia and Souza Filho 2012b, Asadzadeh and de Souza Filho 2016, Kühn, Oppermann, and Hörig 2004b, Hörig et al. 2001, Allen and Krekeler 2010). Previous studies on hydrocarbon characterization often used intricate statistical analysis (such as partial least squares regression, neural networks and other similar algorithm), which relies on shapes of the SWIR hydrocarbon spectra features for quantitative and qualitative mapping (Lammoglia and Souza Filho 2012b, Lammoglia and Filho 2011, 2015, Clark et al. 2010, Scafutto and Souza Filho 2016). Similar works on oil slick characterization on varying soil substrate also relies on shapes of SWIR absorption features for hydrocarbon characterization, using mathematical ratios and algorithms (Asadzadeh and de Souza Filho 2016, Kühn, Oppermann, and Hörig 2004a, Hörig et al. 2001). Some spectra indexes have also been used that considered the reflectance contrast at VNIR and waveform parameters at SWIR for both detection and quantification (Françoise et al. 2021, Kühn, Oppermann, and Hörig 2004b, Loos et al. 2012, Lennon et al. 2005, Li et al. 2012) These works addressed mainly detection and quantification on water and little or no focus on qualitative evaluation of hydrocarbon oil and with consideration to different background substrates. Most of these works also require high resolution data to achieve hydrocarbon characterization and therefore limit the use of moderate resolution multispectral data for spill and seep study. In this paper, we introduce Hydrocarbon Spectral Slope (HYSS), which is a spectra ratio that captures two most obdurate key hydrocarbon spectral features at SWIR (1.73µm and 2.30µm) to quantify and discriminate hydrocarbon oil types on different substrates. This study demonstrates the potential of this spectral index for characterization of hydrocarbons on both very high and moderate spectral resolution data. Since HYSS uses limited spectral input, detailed shapes of key hydrocarbon diagnostic features are no longer important for

analysis, hence its applicability for use on multispectral data. This method requires only two spectral channels in the SWIR region for oil slick characterization and does not need laboratory calibration of oil slick field samples. This spectra index therefore reveals potential of both hyperspectral and multispectral satellite sensors as a future tool for fast broad search and monitoring of oil spill and seep.

Multispectral data are free (from European Space Agency: ESA and National Aeronautics Space Administration: NASA) but there are limited use of these data for oil slick quantitative and qualitative evaluation of hydrocarbon spill or seep in literature and in practice. However, multispectral sensors provide data of higher spatial and temporal coverage, useful for monitoring of large to moderate size spills and seeps. Despite the stated drawback of this sensor category, Advanced Spaceborne Thermal Emission and Reflection Radiometer (ASTER) data demonstrate good potential for estimating the American Petroleum Index (API) gravity and relative exposure time of hydrocarbon oil on ocean seepage (Lammoglia and Filho 2015, Lammoglia and Souza Filho 2012a). Also, Asadzadeh and de Souza Filho (2016) have shown the potential of worldview 3 (WV-3) for direct oil slick detection. Furthermore, Sun et al. (2016), detected an oil slick with 50% pixel fractional coverage by convolving Airborne Visible/Infrared Imaging Spectrometer (AVIRIS) data with Land Satellite (LANDSAT) and Medium Resolution Imaging Spectrometer (MERIS) resolution obtained from the 2010 Deep Water Horizon spill (DWH) in the Gulf of Mexico. At present, spectral resolution of operational multispectral sensors are insufficient to resolve the spectral shape of hydrocarbon oil absorption features. However, the proposed HYSS index harnesses the inherent subtle differences in hydrocarbon absorption maxima by creating a slope between key and persistent spectral features in the SWIR. Previous authors use hydrocarbon feature absorption depth for its quantification and characterization (Clark et al. 2010, Kühn, Oppermann, and Hörig 2004b, Correa Pabón and Souza Filho 2016). This study demonstrates the effectiveness of the proposed spectral index (HYSS) for quantitative and qualitative evaluation of hydrocarbon oils for both high and moderate resolution data, such as those obtainable from hyperspectral and multispectral satellite sensors, while using high spectra resolution data (ASD and AVIRIS) as a precursor. HYSS uses the two prominent hydrocarbon absorption features in the SWIR at 1.73µm and 2.30µm. Absorption features at these wavelength positions occur in all common hydrocarbon oils and are persistent on most background substrates and against oil weathering (Allen and Krekeler 2010, Correa Pabón and Souza Filho 2016). In this article, quantitative evaluation of hydrocarbon is defined as a relative estimation of different classes of oil abundance in oil slick emulsion while qualitative evaluation is meant to discriminate hydrocarbon oil types. The objective is to increase the numbers of sensors for rapid response in oil spill and seep events, for both preliminary pollution monitoring and exploration surveys.

HYSS relies on measuring absorption depth which changes with oil types and thickness. Oil often forms an emulsion with water, in ocean spill events, leading to oil weathering (Daling and StrØm 1999, Mishra and Kumar 2015). Therefore, the spectral response of an oil slick is largely the response from oil emulsion (Svejkovsky et al. 2016). The abundance of surface oil can be measured by two major parameters 1) oil slick thickness 2) and its emulsion state in term of oil-water ratio (Clark et al. 2010). These parameters respond similarly on the spectral curve of an oil slick. In this study, we modelled relative oil abundance by its spectral response to oil-water ratio and thickness. Oil-water ratio with higher oil content often has higher reflectance while those with lesser oil have low reflectance, same with oil thickness (Clark et al. 2010, Lammoglia and Filho 2011). The physics behind this phenomenon is a light scattering and consequence light-loss in oil emulsion of varying thickness and composition (Clark and Roush 1984). As explained by Clark et al. (2010), the variation on scattering of light in oil emulsion is resulted from difference in oil-water ratio, which in turn, result in wide range of spectral shapes of oil slick. The light-loss dependent in the NIR therefore revealed different oil-water ratio and different thickness as varying absorption depth and shapes. Figure 1 shows the discrimination of oil emulsions at different oil-water ratios as depicted by Clark et al. (2010). The slope formed between absorption depths at 1.73µm and 2.30µm characterizes different oil abundance classes. These prominent absorption features are present in all hydrocarbons with an alkane component and are persistent at different weathering states, in mixtures, and against different background substrates (Kühn, Oppermann, and Hörig 2004b, Allen and Krekeler 2010, Correa Pabón and Souza Filho 2016, Lammoglia and Filho 2011).

2. Materials and Method

2.1 Data

Two different datasets are used to demonstrate the qualitative and quantitative discriminating power of HYSS. First, United States Geological Survey (USGS) library spectra of the AVIRIS data of oil-water ratio of DWH spill obtained by Clark et al. (2010) was used for the quantitative discrimination. These spectra represent different classes of oil – water ratios at different thicknesses, further discussed in section 2.1.1 Qualitative discrimination between different crudes and refined oils was demonstrated using laboratory spectra obtained by Allen and Krekeler (2010). These data contain spectra of common crude and refined oils on different common substrates, as further discussed in section 2.1.2

2.1.1 Library spectra of oil-water ratio

At sea, varying states of emulsion formed by crude oil exhibits physical expression and have been characterized by spectroscopy in previous works (Aske, Kallevik, and Sjöblom 2002, ASCE 1996, Daling and StrØm 1999, Mishra and Kumar 2015). Likewise, the changes in its emulsion state have been shown to significantly impact the reflectance and the waveform of hydrocarbon diagnostic features of the oil slick (Lammoglia and Filho 2011). Here, we use AVIRIS spectra of oil-water ratio from Clark et al. (2010) , to quantify the oil abundance on water. These ratios are prepared through dehydration and rehydration, followed by mixing of proportionate amount of DWH oil slick samples with site water samples and are available as part of the USGS spectra library version 7. Details on the emulsion sample preparation and the spectra measurement procedures can be found in this literature. The available oil-water ratio spectra in the USGS library version 7 dataset are: 01:99, 23:77, 40:60, 60:40, 75:25, and 92:08. Except for 01:99 and 75:25, the other classes have a consistent thickness range between 0.05mm to 4mm. Class 1:99 has 28mm thickness and foam, while class 75:25 has 8mm thickness. Class 23:77, 40:60 and 60:40 also have 8mm thickness, which were included in the preliminary stage of the analysis. Class 23:77 and 60:40 have 0.025mm thickness value while other oil – water ratio categories does not and therefore, data for this thickness value are also excluded in the analysis. Since oil spectra are also sensitive to thickness value, data from the four classes of oil-water ratio (oil abundance) are further divided into four available consistent thickness classes 23:77, 40:60, 60:40 and 92:08.

2.1.2 Laboratory spectra of crudes and refined oils

Laboratory data collected by Allen and Krekeler (2010) were used to demonstrate the discriminating power of the proposed

HYSS for different hydrocarbon-substrate combinations. These data were acquired with ASD Field Spec™ Pro-FR2 and comprise four different crude oils and three different refined oils. The oil samples are of types, refined oil and crude oil. Diesel, gasoline and motor oil are the refined oil while heavy, light, intermediate sweet and intermediate sour are the crude oil used with 19.6, 42.2, 32.2, 30.3 API respectively, Intermediate Sweet Intermediate Sour Crude oil have 0.4% and 1.8% respectively. Spectra measurement of these oils were taken against ten common substrates. The substrates used are asphalt, bentonite, a calcareous sand, calcite-dolomite crushed aggregate, concrete, gypsum, a soil with high (2.9%) organic content, Ottawa sand, a quartzitic beach sand, and senescent grass with underlying soil. The senescent grass contain underlying leaf litters and soil. However, for the purpose of this study, all spectral measurements on petri dishes are excluded from this study because they are highly transmissive and are not a naturally occurring background material. Further details on the laboratory set-up and scope of data collection can be found in Allen and Krekeler (2010).

2.2 Hydrocarbon Spectra Slope Index

Hydrocarbon Spectra Slope (HYSS) is the ratio of the difference in reflectance at diagnostic absorption band at SWIR (1.73µm and 2.30µm) of hydrocarbon oil to the difference in the corresponding wavelength interval. This ratio is represented by a negative slope within these diagnostic features as indicated on figure 1. The slope value is an inflection of the maximum depth of these absorption features which also reflect the light loss differentiation by hydrocarbon oil and the chemistry of the oil-water ratio and oil type. Therefore, a proxy for hydrocarbon quantification and discrimination parameters. As Figure 1 shows, both oil and water are highly absorptive at 2.30µm ($\rho < 0.08$ & <0.02, respectively).

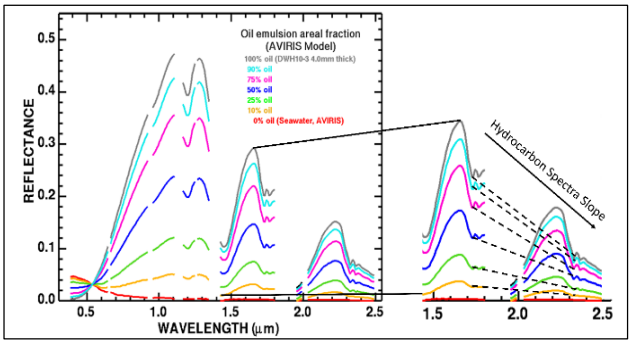

Fig. 1. Spectral profile of oil abundance classes and its relevance to Hydrocarbon Spectra Slope (HYSS). Hydrocarbon slopes are formed between 1.73µm and 2.30µm absorption depth. (Modified after Clark et al, 2010)

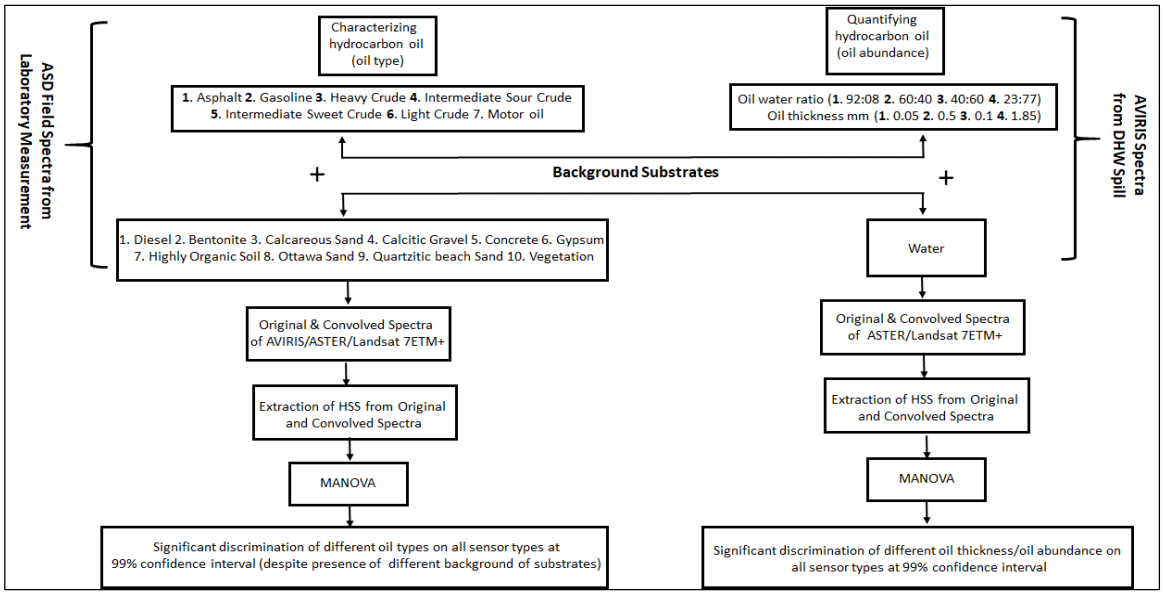

Fig. 2. Flow chart of methodology

In this research, we use obdurate hydrocarbon absorption maxima at 1.73µm and 2.30µm (or the nearest available channel to both for multispectral sensors) for quantification of oil abundance and qualitative characterization of hydrocarbon types on different background substrates. The HYSS evaluation is divided into two parts, quantitative and qualitative computation of corresponding datasets described in section 2.1.1 The flow chart in Figure 2 show an overview of the methodology adopted in this study.

In order to demonstrate the discriminating power of HYSS at different resolutions, the full width half maximum (FWHM) of three different sensors (AVIRIS, ASTER, and Landsat 7 Enhanced Thematic Mapper Plus - ETM+) were used to resample the original ASD spectra for qualitative analysis. We resampled AVIRIS data to ASTER and Landsat 7 bandpasses for oil – water ratio spectra for quantitative analysis. These sensors are commonly used in geo-information science and because their data are freely available. Fortunately, they also have spectral channels that contain or are close to the two hydrocarbon absorption maxima for HYSS. Band 5 and 7 on Landsat 7 contain the hydrocarbon absorption maximum at 1.73µm and 2.30µm, respectively. For ASTER, band 8 contains the 2.30µm feature. ASTER Band 4 (1.60-1.70µm) ends before the 1.73µm feature. In fact, all of the oil-water mixtures reach their maximum SWIR reflectance in this band. Fortunately, as figure 1 demonstrates, there is still a significant gradient, based on oil-water mixture ratios in this range. Furthermore, these two sensors arguably adequate to represent lower bound of other moderate resolution satellite sensors that meet these criteria with higher spectral resolution (such as worldview 3 - WV3).

Whereas multispectral sensors are limited in their ability to measure hydrocarbon-induced absorption features, hyperspectral sensors operating in the SWIR can resolve both the shape and the absorption maxima. The airborne AVIRIS sensor is a useful analog in this respect for both past and future hyperspectral satellite sensors with SWIR coverage (e.g., Hyperion, US;

Environmental Monitoring and Analysis Program–EnMAP, Germany; Hyperspectral Precursor and Application Mission - PRISMA, Italy; Multi-Sensor Micro-satellite Imager –MSMI, South Africa; Hyperspectral Infrared Imager–HyspIRI, USA; Hyperspectral Imager Suite-HISUI ALOS 3, Japan; HYPXIM CA sensor, France, and Geostationary High Resolution Imager – GISAT, India).

3.0 Results and Discussion

3.1 Results

The slope values for oil abundance were calculated for the library spectra (in AVIRIS resolution), discussed in section 2.1.1, and the resampled spectra of ASTER and LANDSAT 7FWHM. The variation of these slope values to different oil abundances classes, on these sensors' FWHM are shown as spectra in Figure 3.1. Bar charts in Figure 4 shows the variation of the oil-water spectra for four different oil abundance classes at four thickness values. Similarly, HYSS values for oil type discrimination were computed from the laboratory spectra of four crudes and three refined oils (section 2.1.2). The lab spectra, along with the resampled spectra for AVIRIS, ASTER, and LANDSAT 7 for Diesel and Heavy Crude on different substrates are shown in figure 3.2. These spectra plots represent measurement of reflectance from different hydrocarbon oil substrate combination.

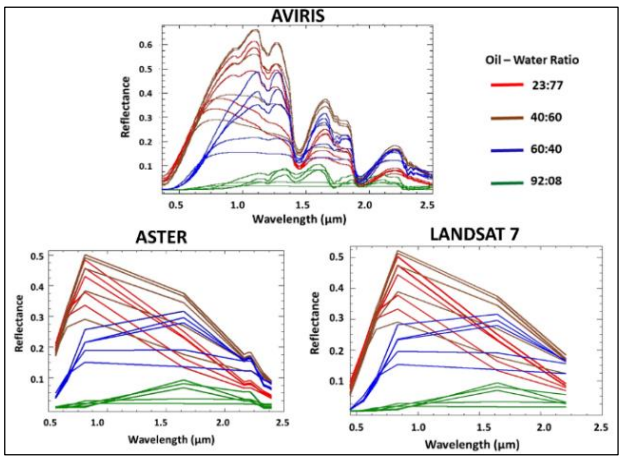

Fig. 3.1 Spectral profile of Oil abundance classes (Oil – Water ratio) in different colour, showing all thickness values in the same colors and at different spectral resolutions for AVIRIS original spectra and convolved spectra for ASTER and LANDSAT 7

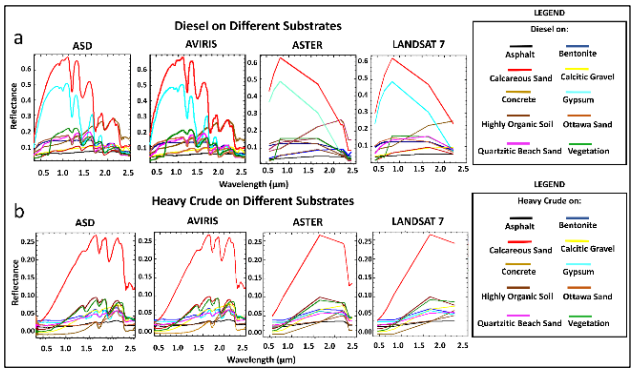

Fig. 3.2. Spectral profile of Hydrocarbon oil-substrates combination a) Diesel b) Heavy Crude, showing the same hydrocarbon oil – substrate combination in the same colors and at different spectral resolutions for original ASD spectra and convolved spectra for AVIRIS, ASTER, and LANDSAT 7 spectra.

The discrimination of oil abundance classes and that of hydrocarbon oil types on different substrates are revealed by both the bar chart and correlation plots. The bar charts show the relative difference in slope value for each oil abundance class and thickness for AVIRIS, ASTER, and Landsat 7 (Figure 4) and each oil type on different substrates for ASD, AVIRIS, ASTER, and Landsat 7 (Figure 6). For each plot (a,b,c,d) in Figure 4, the relative difference of slope value on the bar chart shows apparent separability of oil abundance classes across high (AVIRIS) and moderate (ASTER, Landsat 7) resolution spectral data. In Figure 5, scatter plots of the HYSS value for oil abundance at the four different oil-water thickness values show a linear correlation between the AVIRIS (original data) and ASTER/LANDSAT 7 FWHM. The correlation coefficients ($r2 = 0.94$, p value = 0.001) on this plot suggest a clear discrimination of oil abundance classes (shown by the bubble size), regardless of the spectral resolution, despite the effect of varying oil thickness. Note that the 92:08 ratio group clusters at the upper right of this plot where the slope approaches zero, due to the high absorption by this mixture in both SWIR wavelengths. Similarly, figure 6 shows the bar chart representing relative slope values for different hydrocarbon oil/substrate combinations. Figure 7 shows the correlation plots comparing the ASD measurements to the convolved values for AVIRIS, ASTER, and Landsat 7. These relationships are discussed further in section 3.1.2.

3.1.1 Estimation of Oil abundance

Oil abundance discrimination was analysed across data for all thickness values except that of 4mm thickness. Results for 4mm thickness does not follow general trend of spectral slope values of other oil thickness value. This is probably due to the opacity of this thickness and therefore, minimal scattering of light from the oil fraction. This thickness value is therefore excluded from further analysis. The greyscale bar charts in figure 4 highlight the relative difference in slope value for different oil abundance classes at different thickness (0.05mm, 0.1mm, 0.5mm and 1.85mm) as well as the influence of FHWM resolution and wavelength position of the three sensors involved in this study. The slope values of AVIRIS, ASTER, and LANDSAT 7 are represented as bars with different greyscale values. Although there is an overlap between the reflectance values of the 23:77 and 40:60 ratios, the slopes of all four ratios permit discrimination using HYSS. Figure 3.1 shows spectra of the same oil abundance classes (oil-water ratios) in unique colours (23:77, 60:40, 40:60, and 92:08) while figure 5 shows the correlation of slope values amongst the three sensors. Each circle size represents a different ratio where the largest oil-water ratios are represented as the largest circle. Decreasing oil-water ratios are represented in circles of decreasing sizes. The bar chart shows a general trend of higher slope value with increasing oil abundance across all thickness values when progressing from 40:60 to 60:40 to 92:08. For three thicknesses (0.05, 0.50, 1.85mm), the 23:77 ratio have higher slope value than the 40:60 value. However, bandpasses for each sensor significantly affect the model results. Variation in slope value across oil abundance classes are due primarily due to the differences in the oil content of each abundance classes and are not significantly affected by which sensor is chosen, even for multispectral sensors that do not have a bandpass that intersects precisely with the absorption maxima (e.g., ASTER), as long as there is a bandpass that is spectrally 'nearby', such as ASTER Band 4 (1.60-1.70µm). This bodes well for the use of HYSS with multispectral sensors with SWIR bandpasses that are close, but that do not necessarily contain the hydrocarbon absorption features of interest here. Generally, HYSS discrimination of oil abundance classes are statistically significant at 95% confidence level on all sensors investigated here (p-value <0.001). In summary, FHWM spectral resolution and position affect the slope values but not the discriminative power of the HYSS on the hyperspectral and multispectral sensors involved in this research.

As mentioned above, one notable deviation is the response of 23:77 oil – water slope value in all graphs, as compared to other oil abundance classes except at 0.1mm thickness. This deviation could be as a result of increase sub-pixel mixing of oil and water at low oil content of this class. Note that, the 23:77 oil – water ratio is the oil abundance class with the lowest oil content in the data used for this analysis. This deviation is therefore interpreted as the influence of water spectra over the oil spectra in areal mixing. Conversely, 92:08 oil – water ratio group are clustered at the upper right of the plot can be explain as higher opacity of the largest oil-water ratio, reducing the spectral variation from 1.73 to 2.30µm, resulting in higher HYSS values.

3.1.2 Discrimination of oil types

Figures 6 and 7 plots the bar charts and scatter plots of slope values computed from the original ASD measurement and those computed from resampled AVIRIS, ASTER, and Landsat 7 spectra. In Figure 6, each subplot represent each of the hydrocarbon- substrates combination (e.g., crude and refined oil on ten different substrates).

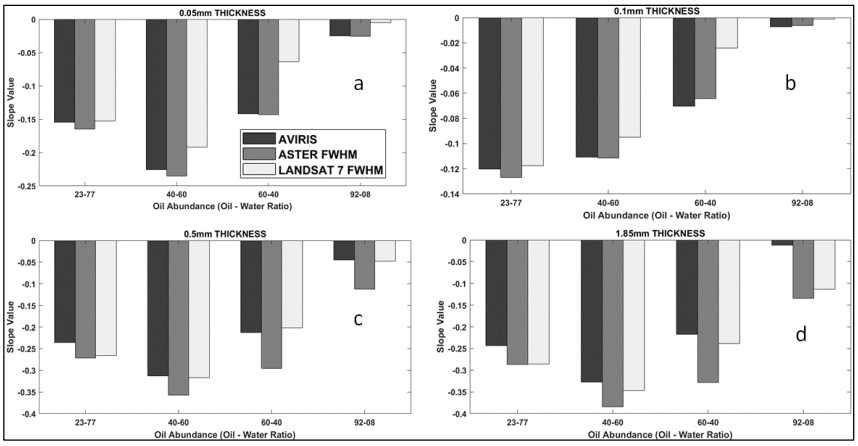

Fig. 4. Bar charts, showing the response of HYSS value for AVIRIS, ASTER, and Landsat 7 at different thickness value; a) 0.05mm, b) 0.1mm, c) 0.5mm, and d) 1.85mm

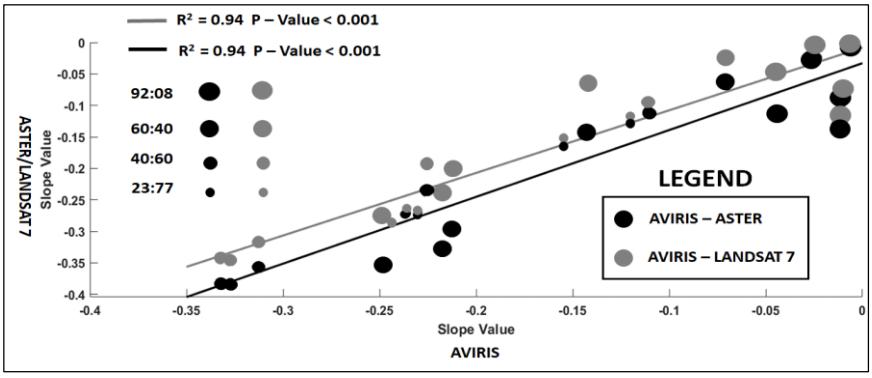

Fig. 5 Correlation of HYSS values for Oil Abundances, as measured by different sensor

Each bar each represent slope value from the original ASD, as well as slope value from convolved spectra for AVIRIS, ASTER, and Landsat 7. Regardless of the substrate types, each hydrocarbon oil sample is discernible based on their slope values, even for partially (e.g., light crude) or highly (i.e., the three refined products) transparent in the SWIR at thicknesses similar to the oil-water ratios, permitting substrate spectral features to influence results. Figure 7 shows the correlation plot of combined slope values for all hydrocarbon-substrates for all sensors shown in figure 6. Due to spectral mixing of some substrates, slope value of hydrocarbon oil are notable affected. Particularly, calcareous sand, Ottawa sand, calcitic gravel, concrete, gypsum, quartzitic beach sand, and vegetation significantly influence HYSS values for the resampled spectra at multispectral resolution (blue = ASTER, green = Landsat 7), showing as deviation from linearity on the correlation plot (indicated with black rings on plot in figure 7). This deviations is due to coarse spectra sampling of the multispectral sensors with respect to hydrocarbon diagnostic absorption bands used in HYSS and non-conformity to these absorption maxima. This is scenario is accentuated on Landsat 7 spectra, with deviations resulting to zero and positive slope values, as shown in Figure 6a, 6c, 6d and 6g). Note that slope values for AVIRIS (red symbols in figure 7) is rather very linear, depicting a strong potential for characterizing hydrocarbon on hyperspectral data using slope value. This is not unexpected for sensor with fine resolution which also conform precisely to wavelength positions of hydrocarbon diagnostic features that defined the slope value. Most of the deviation is below a linear fit to the data, implying stronger than expected HYSS values, which indicates greater differences in reflectance at 1.73 and 2.30µm than expected. The gypsum and calcareous sand substrates showed strong deviation, mainly due to a great difference (-0.25) in reflectance between 1.73 and 2.30µm, however all other substrates have reflectance values less 0.10. Both quartzitic susbstrate exhibit very high transmission, particularly the Ottawa sand, showing stronger than normal hydrocarbon absorption features, and consequently, higher than expected HYSS values (Raveia et al. 2008, Satterwhite and Allen 2005). This difference persists on hydrocarbon-substrate combination due to some measure of transmission for all hydrocarbon samples except for heavy crude and intermediate sour crude at 1.73µm and nearly no transmission by any hydrocarbon oil at 2.30µm. These

hydrocarbon (asterisks and downward triangles, respectively) are notably outliers by producing lower than expected slope values, fundamentally due to this lack of transmission and consequential near opacity at 1.73µm. Hydrocarbon with relatively higher transmissions at 1.73µm, such as diesel (circles), motor oil (boxes), light crude oil (diamonds), intermediate sweet crude oil (sideways triangles) produced higher than expected slope values. In order to evaluate the trend of variation of slope values across hydrocarbon-substrates combination, we used MANOVA to determine separability of hydrocarbon oil samples from one another.

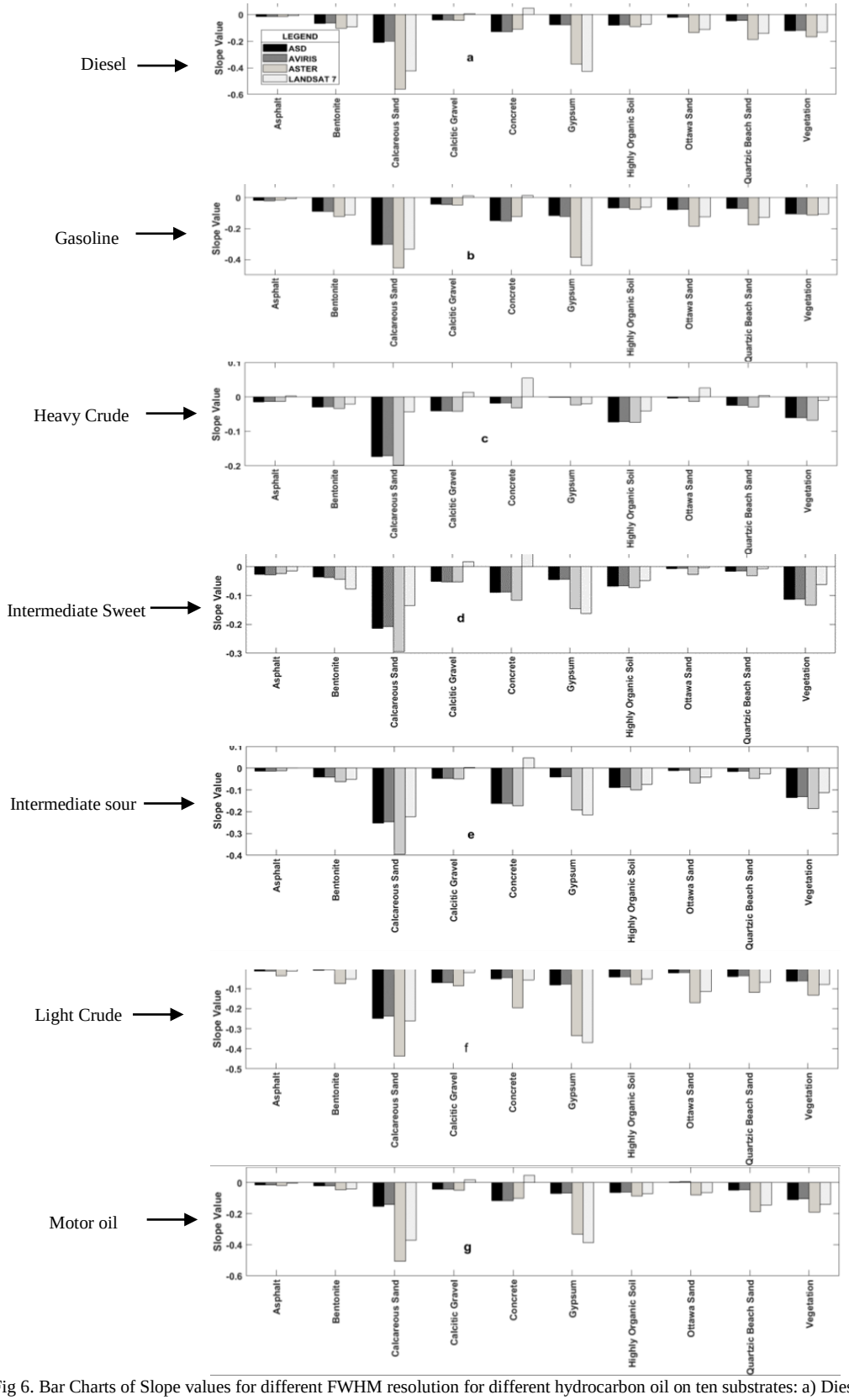

Fig 6. Bar Charts of Slope values for different FWHM resolution for different hydrocarbon oil on ten substrates: a) Diesel, b) Gasoline and c) Heavy Crude d)Intermediate Sweet Crude e) Intermediate Sour Crude f) Light Crude g) Motor oil

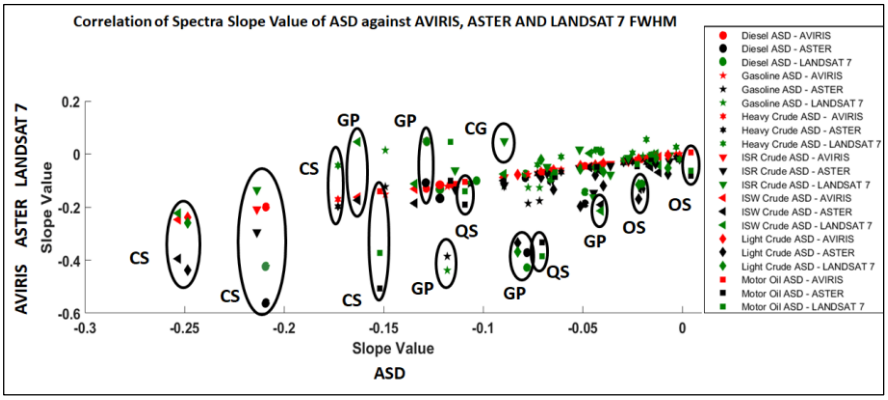

Fig. 7. Correlation of HYSS values for all hydrocarbon on different substrates at different resolution, showing the linearity of ASD measurements and slope value from convolved AVIRIS. Note the deviation from linearity of slope value from convolved ASTER, and Landsat 7 due to the spectral response of substrates (Calcareous Sand -CS, Ottawa Sand-OS, Quartzitic Sand –QS, Calcitic Gravel -CG and Gypsum -GP)

Table 1 shows correlation value and corresponding p value for each hydrocarbon-substrates combination for each of the sensors compared to the ASD lab spectra. As mentioned above, HYSS value for AVIRIS hew very strongly to the lab spectra, which is expected for a hyperspectral sensor that can measure absorption maxima with precision of ≤10 nm and with a bandpasses in the spectral range of these absorption features. On the contrary, multispectral sensors have lower correlation coefficient and P- values. This is particularly true for results from Landsat 7, none of which reaches a R value of 0.80. Relatively, ASTER has a number of high (>0.80) R values and low p values (<0.01), due to conformity of its bandpass to 2.30µm wavelength position.

Table 1. Correlation Coefficient and P - Values of HYSS value of different hydrocarbon-substrate combination at different resolution

Oil – Water Ratio/ Thickness	Sum of Squares	Df	Mean Square	F-Ratio	P-Value
Oil – Water Ratio	0.408	3	0.136	19.794	0.000
Thickness	0.288	4	0.072	7.859	0.000
Sensor Resolution	0.021	2	0.011	0.780	0.463

These poor values are a reflection of the relatively broad spectral range of Landsat 7's SWIR bands and the dynamic nature of both the hydrocarbon oils, as well as some of the substrates over these large bandpasses (≥0.20µm). This explained why slope value changes from negative to positive values on some hydrocarbon-substrates combination (see figure 6). As a result, both the R and P value for the affected plots are considerably lower than they are for ASTER (indicated with downward arrow in table 1).

3.1.3 Statistical Analysis of the Results

A Multifactor Analysis of Variance (MANOVA) was used to test the significant difference of hydrocarbon slope value as a bases for quantitative discrimination of the oil abundance classes and the discrimination of hydrocarbon oil types. The results showed a significant value for both analysis at 99% confidence level (see tables 2 and 3). Discrimination of oil abundance classes and those of hydrocarbon oil types by slope value are highly significant with p value < 0.01 at resolution for ASD, AVIRIS, ASTER and LANDSAT 7. All abundance classes are significantly distinguishable at 99% confidence level, based on their slope value at all thickness value (p value= 0.000) and Oil-water ratio (p value= 0.00) and at all resolution (p value = 0.463). This implies that HYSS successfully distinguishes all different oil abundance classes as well as its varying thickness values. That is, hydrocarbon spectral slope values are not significantly different at the resolution of the three sensors. In other words, these three sensors were able to distinguish oil abundance classes and thickness ranges. Similarly, all slope values from the original ASD data and resample spectra were statistically significant at 95% confidence level (p value < 0.01) for the qualitative analysis. All hydrocarbon–substrate combinations investigated in this research have high significance at 95% confidence level at all resolution (see table 3). HYSS value for hydrocarbon oils investigated are significantly distinguishable at all spectral resolutions, despite the broad spectral bandpasses of ASTER and LANDSAT 7, as shown on the correlation plots (figure 7) and that of quantitative analysis of oil abundance (figure 5).

Table 2: ANOVA of Slope Value for oils abundance (oil _ water ratio) and thickness against spectral resolution

Oil types	Coefficient of Correlation (R) and P - Value		
Resolution	ASD – AVIRIS	ASD – ASTER	ASD – LANDSAT 7
Diesel	0.99 / <0.001	0.73 / 0.016	0.49 / 0.148 ↓
Gasoline	0.99 / <0.001	0.80 / 0.005	0.57 / 0.080
Heavy Crude	0.99 / <0.001	0.99 /<0.001	0.61 / 0.061
Intermediate Sour Crude	0.99 / <0.001	0.93 /<0.001	0.40 / 0.248↓
Intermediate Sweet Crude	0.99 / <0.001	0.89 /<0.001	0.40 / 0.245↓
Light Crude	0.99 / <0.001	0.84 / 0.002	0.60 / 0.069
Motor Oil	0.99 / <0.001	0.71 / 0.020	0.47 / 0.172↓

Table 3: Multifactor ANOVA of HYSS Value for Hydrocarbons oils against spectral resolution and substrates

Hydrocarbon on Substrates	Sum of Squares	Df	Mean Square	F-Ratio	P-Value
Diesel on Substrate	0.372	9	0.041	4.949	0.000
Resolution	0.068	3	0.023	1.478	0.237
Gasoline on Substrates	0.382	9	0.042	9.065	0.000
Resolution	0.028	3	0.009	0.687	0.566
Heavy Crude on Substrates	0.070	9	0.008	8.662	0.000
Resolution	0.015	3	0.005	2.162	0.109
Intermediate Sour Crude on Substrates	0.131	9	0.015	8.605	0.000
Resolution	0.013	3	0.004	0.890	0.456
Intermediate Sweet Crude on Substrates	0.234	9	0.026	8.892	0.000
Resolution	0.021	3	0.007	0.846	0.478
Light Crude on Substrates	0.272	9	0.030	6.103	0.000
Resolution	0.074	3	0.025	2.550	0.071
Motor Oil on Substrates	0.300	9	0.033	4.361	0.001
Resolution	0.066	3	0.022	1.717	0.181

3.2 Discussion of results

Quantitative and qualitative analysis of hydrocarbons mixed with water and on ten different substrates demonstrates the capability of HYSS method for potential hydrocarbon

characterization. HYSS values suggest a significant relative discrimination of oil slick abundance classes (both in terms of oil-water ratio and thickness) and discrimination of different hydrocarbon oils on varieties of substrates at 99% confidence level across the datasets used in multifactor analysis of variance. Furthermore, the observed difference in slope value of the oil abundance classes and that of the hydrocarbon-substrates discrimination are statistically significant, with p values lower than 0.01 significance level (tables 2 and 3). For oil abundance class discrimination, statistical significance is higher than 99% confidence level at all resolution (p value = 0.000, 0.000, and 0.463). For qualitative analysis, comparing slope value from the original ASD data to corresponding slope values from resampled spectra reveal the bandpass location, and effect of highly reflecting substrates, particularly calcareous sand, Gypsum, and quartzitic sands produce slope values that deviate from expected linear spectral response in correlation plot (figure 7). However, HYSS values for oil abundance classes and hydrocarbon-substrates analyzed in this research are statistically significant for discrimination at all sensors' FHWM resolution. These results indicate that multispectral and hyperspectral sensors are potentially useful tools for mapping hydrocarbons, even on a wide-ranging substrates. The discriminative ability of HYSS can be explained on a molecular scale by the model's sensitivity to subtle changes in hydrocarbon absorption depths at C-H overtone and combination bands in the SWIR (Cloutis 1989). The changes in absorption depths reflect overlapping hydroxyl (OH-) and C-H transmission and absorption, mixed in the multiple ratios outlined above. For the qualitative discrimination of hydrocarbon oil types, HYSS ability to differentiate oils and refined products is a function primarily of differing transmission values for each hydrocarbon oil, as well as the underlying substrate's reflectance. Other factors, such as absorption maxima at values different than 1.73µm (e.g., gasoline) and differing asymmetric absorption feature shapes (e.g., triplets (gasoline) vs doublets (all other samples) are also likely contributors, although the relative impacts merit additional study.

The observed deviation of the HYSS value in the 23:77 oil – water ratio sample and from the resampled spectra are also explainable with high water content of this oil abundance class. The 23:77 oil abundance class has the highest water content. Water is highly absorptive in the SWIR so volume scattering from the oil which reaches the water is strongly absorbed, resulting in lower contrast between reflectance values at 1.73 and 2.30µm than in the other samples. Also, due to sub optimal band pass and relatively broad spectral ranges, ASTER and LANDSAT 7 do not have spectral bands that coincide precisely with the key hydrocarbon bands used by the slope model (i.e., 1.73µm and 2.30µm). Therefore, the input response from the inappropriate spectra channels during resampling is also another cause of slope value variation observed from resampled spectra.

As observed in previous studies, result from HYSS showed that quantitative and qualitative analysis of hydrocarbon oil on varying substrates can be ambiguous, due to the high transmissivity of some hydrocarbons in the shorter SWIR region, combined with the interference from key spectral bands of substrates (Scafutto and Souza Filho 2016, Allen and Krekeler 2010). The complex interference of spectra of hydrocarbon oil-substrate investigated (as indicated in figure 6 and 7) influenced the resulting HYSS value but all hydrocarbon oil types were significantly discriminated across all substrates used in this research (see table 3). Even on highly reflecting substrates, HYSS demonstrates a significant discriminative tendency for all studied hydrocarbon oil –substrates combination, even at resampled scales of multispectral sensors with sub-optimal bandpasses. That is, each hydrocarbon-substrate combination as well as oil abundance/thickness classes have significantly different slope value sufficient for discrimination.

It is worthy to note limitations of this study for further works on the proposed HYSS spectral index. Laboratory spectra and AVIRIS spectral were used as a precursor to model response of multispectral image which depend also on other image parameters such spatial/radiometric resolution and dynamic range. Although, it is adequately justified to infer that these image parameters for hyperspectral data of AVIRIS specification or higher will perform optimally with HYSS spectra index as predicted by this model. However, the effect of other image parameters on multispectral image for this spectra ratio should be investigated. On AVIRIS spectra, effect of high water content (23:77) and higher oil content (92:08) lower the response of HYSS spectra index for quantification but still with significant discrimination. The former is most likely due to the effect of water in spectral mixing while the later could be effect of opacity of crude oil to light and non-differentiation of value thickness value in analysis because of limited data volume (Clark and Roush 1984). In oil type discrimination on substrates, effect of moisture content of background substrates on HYSS were not investigated and therefore merit further study. Potential impact of HYSS spectra index and contribution to knowledge of hydrocarbon mapping is the possibility of achieving fast computational assessment in spill and seep events. This is owing to the reliance of this simple spectral index on depth of absorption maximum of two most obdurate channels at SWIR (1.73µm and 2.30µm), which are direct response to chemical changes in hydrocarbon chemistry (Clark et al, 2009).

Similar spectral parameters proposed for thickness discrimination used contrast of reflectance at NIR region (490nm to 885nm) on oil spectra on hyperspectral and multispectral data (Lennon et al, 2005, Loos et al, 2012). Li et al, 2012 also used a similar spectral index which uses radiance contrast of Spec TIR hyperspectral data at NIR (580nm to 748nm). Obviously, these spectral index in previous studies enhance the contrast in reflectance/radiance at NIR, to discriminate oil thickness. In contrast, parameter for spectral index used in HYSS is maximum absorption depth at SWIR, from key and obdurate diagnostic features of hydrocarbon oils, which may not only relate to differences in thickness/oil-water ratio but also oil types as indicated in this study. Absorption depth of these diagnostic feature are indicative of oil chemistry, chemical changes and physics of light loss differentiation for thickness measure (Clark et al 2009; Clark et al, 2010, Clark and Roush 1984). Similar to HYSS, Hörig et al. (2001), Kühn, Oppermann, and Hörig (2004b) and Francoise et al, 2021 used spectra indexes by considering absorption depth at 1.7µm and 2.3µm for hydrocarbon characterization. Hörig et al. (2001) and Kühn, Oppermann, and Hörig (2004b) focused on detection of hydrocarbon on polluted soil using spectral index derived from waveform parameter at these wavelength on hyperspectral data. Françoise et al. (2021) proposed a spectral index for hydrocarbon characterization on water, using absorption maximum at 1.7µm, 2.3µm and 2.6µm. Unlike HYSS, this method does not depend only on oil spectral for oil characterization but also uses other oil slick parameters from extensive database from separate experiments. Also, spectral ratio from the study does not demonstrates discrimination of hydrocarbon oil any other different substrate other than water. HYSS presents a simple spectral index that uses only two obdurate absorption maximum for hydrocarbon for potential characterization across range of common background substrates, with potential for rapid broad range search for spill/seep.

4. Conclusion

This study have demonstrated the potential of HYSS for hydrocarbon quantification and characterisation with both hyperspectral and multispectral sensors. Discrimination of oil abundance and oil types achieved on all studied hydrocarbon oil-substrate combinations are statistically significant at 99% confidence interval. As expected, HYSS performs especially well on hyperspectral data such as ASD lab instrument or AVIRIS measurement that capture key hydrocarbon spectral features. While multispectral sensors such as ASTER and LANDSAT 7 do not possess sufficiently fine resolution to resolve these key hydrocarbon spectral bands, quantitative and qualitative characterization is still statistically significant with varieties of substrates. Highly reflective and transmissive substrates exhibit a spectra response that produce results that deviate from the linear responses seen in the ASD and AVIRIS data, which may limit HYSS on such substrates. However, this method offers a relative quantification and characterization of hydrocarbon oil that can be deployed for broad area search particularly for mapping land and water based oil spills and seeps with hyperspectral and multispectral data. In subsequent efforts, we anticipate assessing the utility HYSS for hydrocarbon quantification and characterization using imagery data. This is particularly necessary to assess the effect on HYSS spectra index due to other image parameters not considered in this study, such as spatial resolution, radiometric range, bidirectional reflectance and detection limits of common hyperspectral and multispectral sensors.

Acknowledgement

The Authors thank Tetfund for the scholarship for this research. Spectra data of oil – water ratio were obtained from the spectra library version 7 from USGS online archive. The crude oil samples used by Allen and Krekeler (2010) were provided by ExxonMobil.

References

Allen, and Krekeler. 2010. "Reflectance spectra of crude oils and refined petroleum products on a variety of common substrates." Active and Passive Signatures.

Andreou, Charoula, and Vassilia Karathanassi. 2011. "Endmember detection in marine environment with oil spill event." Image and Signal Processing for Remote Sensing XVII.

Asadzadeh, Saeid, and Carlos Roberto de Souza Filho. 2016. "Investigating the capability of WorldView-3 superspectral data for direct hydrocarbon detection." Remote Sensing of Environment 173:162-173. doi: http://dx.doi.org/10.1016/j.rse.2015.11.030.

ASCE. 1996. "State of the art review of modeling transport and fate of oil spill (Task Committee on Modeling Oil Spills of the Water Resources Engineering Division)." Journal of Hydraulic Engineering, 122, :594–609.

Aske, Narve, Harald Kallevik, and Johan Sjöblom. 2002. "Water-in-crude oil emulsion stability studied by critical electric field measurements. Correlation to physico-chemical parameters and near-infrared spectroscopy." Journal of Petroleum Science and Engineering 36 (1):1-17. doi: https://doi.org/10.1016/S0920-4105(02)00247-4.

Clark, Roger N, John M Curchin, Todd M Hoefen, and Gregg A Swayze. 2009. "Reflectance spectroscopy of organic compounds: 1. Alkanes." Journal of Geophysical Research: Planets 114 (E3).

Clark, Roger N, Ira Leifer Gregg A. Swayze, K. Eric Livo, Raymond Kokaly, Todd Hoefen,, Michael Eastwood Sarah Lundeen, Robert O. Green, Neil Pearson, Charles Sarture, Ian McCubbin,, and Eliza Bradley Dar Roberts, Denis Steele, Thomas Ryan, Roseanne Dominguez. 2010. "A Method for Quantitative Mapping of Thick Oil Spills Using Imaging Spectroscopy." Open file Report 2010-1167.

Clark, Roger N, and Ted L Roush. 1984. "Reflectance spectroscopy: Quantitative analysis techniques for remote sensing applications." Journal of Geophysical Research: Solid Earth 89 (B7):6329-6340.

Cloutis, E. A. 1989. "Spectral reflectance properties of hydrocarbons: remote-sensing implications." Science 245 (4914):165-8. doi: 10.1126/science.245.4914.165.

Correa Pabón, Rosa Elvira, and Carlos Roberto de Souza Filho. 2016. "Spectroscopic characterization of red latosols contaminated by petroleum-hydrocarbon and empirical model to estimate pollutant content and type." Remote Sensing of Environment 175 (Supplement C):323-336. doi: https://doi.org/10.1016/j.rse.2016.01.005.

Daling, Per S., and Tove StrØm. 1999. "Weathering of Oils at Sea: Model/Field Data Comparisons." Spill Science & Technology Bulletin 5 (1):63-74. doi: https://doi.org/10.1016/S1353-2561(98)00051-6.

Fingas, M., and C. E. Brown. 2017. "Chapter 5 - Oil Spill Remote Sensing." In Oil Spill Science and Technology (Second Edition), 305-385. Boston: Gulf Professional Publishing.

Françoise, Viallefont-Robinet, Roupioz Laure, Caillault Karine, and Foucher Pierre-Yves. 2021. "Remote sensing of marine oil slicks with hyperspectral camera and an extended database." Journal of Applied Remote Sensing 15 (2):1-18. doi: 10.1117/1.JRS.15.024504.

Holmes, J. V., G. Graettinger, and I. R. MacDonald. 2017. "Chapter 17 - Remote Sensing of Oil Slicks for the Deepwater Horizon Damage Assessment A2 - Fingas, Mervin." In Oil Spill Science and Technology (Second Edition), 889-923. Boston: Gulf Professional Publishing.

Hörig, B., F. Kühn, F. Oschütz, and F. Lehmann. 2001. "HyMap hyperspectral remote sensing to detect hydrocarbons." International Journal of Remote Sensing 22 (8):1413-1422. doi: 10.1080/01431160120909.

Kühn, F, K. Oppermann, and B. Hörig. 2004a. "Hydrocarbon Index – an algorithm for hyperspectral detection of hydrocarbons." International Journal of Remote Sensing 25 (12):2467-2473. doi: 10.1080/01431160310001642287.

Kühn, F, Konstanze Oppermann, and Bernhard Hörig. 2004b. "Hydrocarbon Index–an algorithm for hyperspectral detection of hydrocarbons." International Journal of Remote Sensing 25 (12):2467-2473.

Lammoglia, Talita, and Carlos Roberto de Souza Filho. 2011. "Spectroscopic characterization of oils yielded from Brazilian offshore basins: Potential applications of remote sensing." Remote Sensing of Environment 115 (10):2525-2535. doi: http://dx.doi.org/10.1016/j.rse.2011.04.038.

Lammoglia, Talita, and Carlos Roberto de Souza Filho. 2015. "Chronology and backtracking of oil slick trajectory to source in offshore environments using ultraspectral to multispectral remotely sensed data." International Journal of Applied Earth Observation and Geoinformation 39:113-119. doi: http://dx.doi.org/10.1016/j.jag.2015.03.007.

Lammoglia, Talita, and Carlos Roberto de Souza Filho. 2012a. "Mapping and characterization of the API gravity of offshore hydrocarbon seepages using multispectral ASTER data." Remote Sensing of Environment 123 (Supplement C):381-389. doi: https://doi.org/10.1016/j.rse.2012.03.026.

Lammoglia, Talita, and Carlos Roberto de Souza Filho. 2012b. "Mapping and characterization of the API gravity of offshore hydrocarbon seepages using multispectral ASTER data." Remote Sensing of Environment 123:381-389. doi: http://dx.doi.org/10.1016/j.rse.2012.03.026.

Lennon, Marc, Sergey Babichenko, Nicolas Thomas, Vincent Mariette, and Grégoire Mercier. 2005. "Combining passive hyperspectral imagery and active fluorescence laser spectroscopy for airborne quantitative mapping." 4th EARSEL Workshop on Imaging Spectroscopy, Warsaw, Poland.

Li, Q., L. Lu, B. Zhang, and Q. Tong. 2012. "Oil Slope Index: An algorithm for crude oil spill detection with imaging spectroscopy." 2012 Second International Workshop on Earth Observation and Remote Sensing Applications, 8-11 June 2012.

Liu, Bingxin, Ying Li, Qiang Zhang, and Liang Han. 2016. "Assessing sensitivity of hyperspectral sensor to detect oils with sea ice." Journal of Spectroscopy 2016.

Loos, E., L. Brown, G. Borstad, T. Mudge, and M. Álvarez. 2012. "Characterization of oil slicks at sea using remote sensing techniques." 2012 Oceans, (pp. 1-4). IEEE, 14-19 Oct. 2012.

Lu, Yingcheng, Qingjiu Tian, Xinyuan Wang, Guang Zheng, and Xiang Li. 2013. "Determining oil slick thickness using hyperspectral remote sensing in the Bohai Sea of China." International Journal of Digital Earth 6 (1):76-93. doi: 10.1080/17538947.2012.695404.

Mishra, Aditya Kumar, and G. Suresh Kumar. 2015. "Weathering of Oil Spill: Modeling and Analysis." Aquatic Procedia 4:435-442. doi: http://dx.doi.org/10.1016/j.aqpro.2015.02.058.

Raveia, Mary Adelina, Sarah B Hendrickson, John T Fitzgerald, Mark PS Krekeler, and Lance E Kearns. 2008. "Investigations of impurities of the Ottawa standard sand." Annual Meeting of the Geological Society of America Abstracts with Programs.

Reséndez-Hernández, Laura A., Daniel Prudencio-Csapek, and Diego Fabián Lozano-García. 2018. "Hyperspectral analysis of soil polluted with four types of hydrocarbons." Geocarto International:1-18. doi: 10.1080/10106049.2018.1451921.

Satterwhite, Melvin B, and C Scott Allen. 2005. "Reflectance spectra and optical depth of some sandy soils." Algorithms and Technologies for Multispectral, Hyperspectral, and Ultraspectral Imagery XI.

Scafutto, Rebecca Del'Papa Moreira, and Carlos Roberto de Souza Filho. 2016. "Quantitative characterization of crude oils and fuels in mineral substrates using reflectance spectroscopy: Implications for remote sensing." International Journal of Applied Earth Observation and Geoinformation 50 (Supplement C):221-242. doi: https://doi.org/10.1016/j.jag.2016.03.017.

Sun, Shaojie, Chuanmin Hu, Lian Feng, Gregg A. Swayze, Jamie Holmes, George Graettinger, Ian MacDonald, Oscar Garcia, and Ira Leifer. 2016. "Oil slick morphology derived from AVIRIS measurements of the Deepwater Horizon oil spill: Implications for spatial resolution requirements of remote sensors." Marine Pollution Bulletin 103 (1):276-285. doi: https://doi.org/10.1016/j.marpolbul.2015.12.003.

Svejkovsky, Jan, Mark Hess, Judd Muskat, Tim J. Nedwed, Jenifer McCall, and Oscar Garcia. 2016. "Characterization of surface oil thickness distribution patterns observed during the Deepwater Horizon (MC-252) oil spill with aerial and satellite remote sensing." Marine Pollution Bulletin 110 (1):162-176. doi: https://doi.org/10.1016/j.marpolbul.2016.06.066.

Wettle, Magnus, Paul J. Daniel, Graham A. Logan, and Medhavy Thankappan. 2009. "Assessing the effect of hydrocarbon oil type and thickness on a remote sensing signal: A sensitivity study based on the optical properties of two different oil types and the HYMAP and Quickbird sensors." Remote Sensing of Environment 113 (9):2000-2010. doi: https://doi.org/10.1016/j.rse.2009.05.010.